frontiers | Frontiers in Physics

TYPE Original Research
PUBLISHED 05 October 2022
DOI 10.3389/fphy.2022.1009489

OPEN ACCESS

EDITED BY
Pierre Descouvemont,
Université libre de Bruxelles, Belgium

REVIEWED BY
Petr Navratil,
TRIUMF, Canada
Andres Arazi,
Comisión Nacional de Energía Atómica, Argentina

*CORRESPONDENCE
Michael Wiescher,
mwiesche@nd.edu

SPECIALTY SECTION
This article was submitted to Nuclear Physics,
a section of the journal
Frontiers in Physics

RECEIVED 02 August 2022
ACCEPTED 14 September 2022
PUBLISHED 05 October 2022

CITATION
Wiescher M, deBoer RJ and Görres J (2022), Threshold effects in the $^{10}B(p,\alpha)^{7}Be$, $^{12}C(p,\gamma)^{13}N$ and $^{14}N(p,\gamma)^{15}O$ reactions.
Front. Phys. 10:1009489.
doi: 10.3389/fphy.2022.1009489

Threshold effects in the $^{10}B(p,\alpha)^{7}Be$, $^{12}C(p,\gamma)^{13}N$ and $^{14}N(p,\gamma)^{15}O$ reactions

Michael Wiescher*, Richard James deBoer and Joachim Görres

Department of Physics and Astronomy, University of Notre Dame, Notre Dame, IN, United States

The typical energy range for charge particle interactions in stellar plasmas corresponds to a few 10s or 100s of keV. At these low energies, the cross sections are so vanishingly small that they cannot be measured directly with accelerator based experimental techniques. Thus, indirect studies of the compound structure near the threshold are used in the framework of reaction models to complement the direct data in order to extrapolate the cross section into the low energy regime. However, at the extremely small cross sections of interest, there maybe other quantum effects that modify the such extracted cross section. These may result from additional nuclear interactions associated with the threshold itself or could be due to other processes, such as electron screening. Measurements in plasma environments like at the OMEGA or National Ignition Facility facilities offer an entirely new set of experimental conditions for studying these types of reactions, often directly at the energies of interest. In this paper, we examine three reaction, $^{10}B(p,\alpha)^{7}Be$, $^{12}C(p,\gamma)^{13}N$ and $^{14}N(p,\gamma)^{15}O$, which have all been measured at very low energies using accelerator based methods. All three reactions produce relatively long-lived radioactive nuclei, which can be collected and analyzed at plasma facilities using a variety of collection and identification techniques.

KEYWORDS

nuclear plasmas, nuclear reactions, R-matrix, electron screening, nuclear astrophysics

1 Introduction

Nuclear reactions in high density plasma environments in the interior of stars are the engine for the chemical evolution of our universe. The nuclear reaction rates used for simulating the associated nucleosynthesis patterns rely mostly on accelerator based reaction cross section measurements folded with the Maxwell Boltzmann energy distribution of the interacting particles. However, the laboratory cross section data are typically obtained at much higher energies than those that occur in a stellar environment and in most cases the reaction rates rely on theoretical extrapolation into the stellar energy range, the so-called Gamow window. While such extrapolations require a reliable understanding of the nuclear structure near the particle threshold as well of the contributing nuclear reaction components and mechanisms, they also require a reliable understanding of the environmental conditions in the stellar plasma. The latter is not yet available and relies entirely on model predictions [1], which do not

seem to match the available experimental data very well. This requires the development of an experimental program in nuclear reaction studies in a hot plasma environment. The production of a stellar plasma at sufficiently high temperature and density conditions in the laboratory is a unique challenge, but the development of high power laser induced inertial plasma environments seems to provide a path in that direction. First experiments on the study of fusion reactions between different hydrogen and helium isotopes have revealed promising results, but they have focused so far on fusion reactions between low Z isotopes, such as ^{3}H (^{2}H, n)^{4}He [2] or ^{3}H (^{3}H, $2n$)^{4}He [3], and ^{3}He (^{3}H, p)^{5}Li and ^{3}He (^{3}He, $2p$)^{4}He fusion branches [4] where the cross section study is less handicapped by the Coulomb barrier and supported by the strong interaction based fusion mechanism.

Inertial confinement fusion (ICF) [5] facilities like the National Ignition Facility (NIF) [6] and OMEGA [7] endeavour to create an environment similar to that found in a nuclear detonation or in the core of a star, but under highly spatially confined and controlled conditions. This is accomplished by focusing an array of high powered laser beams onto a tiny pellet or capsule of fusion fuel. The radiation pressure causes its rapid implosion achieving for short nano-second time periods temperature and density conditions comparable to stellar plasma conditions [8]. So far nuclear reaction studies at both OMEGA and NIF have not gone beyond the fusion of very light hydrogen and helium isotopes. To explore the value of these facilities for a broader nuclear astrophysics program, it might be appropriate to investigate possible measurements for higher Z isotopes. A first attempt has been made recently to study the ^{10}B(α, n)^{13}N reaction [9] at NIF providing a first glimpse at the challenges such measurements will have to be overcome, both in the collection and in identification of the reactions products [10].

While the cross section of the aforementioned fusion reactions between hydrogen isotopes is rather large, many, if not most, of the reactions of interest to astrophysics are radiative capture processes. They typically have a substantially lower cross section since the Hamiltonian is determined by the electromagnetic and not the strong interaction force. Nevertheless the production and measurement of long-lived reaction products might provide a sufficiently efficient way to directly determine the reaction rate for the temperature and density condition of an inertial fusion plasma.

In the following sections, we will discuss three suggested reactions ^{10}B(p,α)^{7}Be, ^{12}C(p,γ)^{13}N and ^{14}N(p,γ)^{15}O and their role in different stellar environments. We will also present the cross sections anticipated for conditions that can be reached at laser plasma facilities such as OMEGA and NIF. These cross sections are based on extrapolations of accelerator based data using phenomenological R-matrix theory [17, 11]. The R-matrix calculations presented here were performed with the AZURE2 code [13] and are extensions of those described in detail in the works of [13,14], and [15] for the ^{10}B(p,α)^{7}Be,

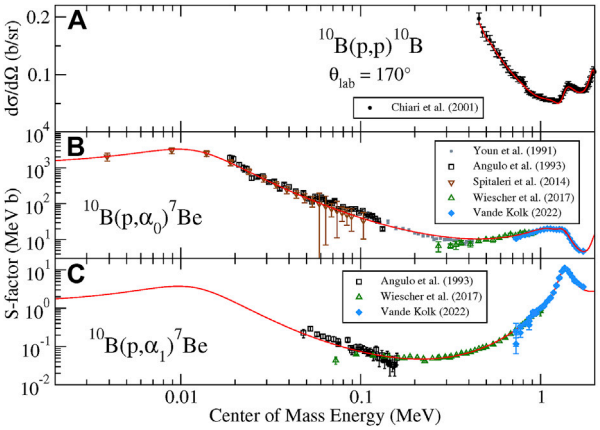

FIGURE 1
Simultaneous R-matrix fits to **(A)** the scattering data of Chiari et al. [20], **(B)** the ^{10}B(p, α_0)^{7}Be (transition to the ground state of ^{7}Be) data of Youn et al. [21], Angulo et al. [22], Wiescher et al. [18], Spitaleri et al. [23], and Vande Kolk et al. [14] and **(C)** the ^{10}B(p, α_1)^{7}Be (transition to the first excited state of ^{7}Be) data of Angulo et al. [24], Wiescher et al. [18], and Vande Kolk et al. [14].

^{12}C(p,γ)^{13}N and ^{14}N(p,γ)^{15}O reactions, respectively. Therefore, only the details relevant to this work are discussed here. The anticipated reaction yield in the laser driven plasma environment will be presented and the feasibility of radiative capture experiments at laser plasma facilities will be estimated and discussed.

2 The ^{10}B(p,α)^{7}Be reaction

The ^{10}B(p,α)^{7}Be reaction plays an important role in the nucleosynthesis of first stars. It effectively reduces the flow of the competing ^{10}B(α,d)^{12}C reaction by which the primordial He and Li can be converted into C, N, and O [16]. On the other hand, it feeds two alternative branches of the hot pp-chains [17], ^{7}Be(e^{-},ν)^{7}Li(α,γ)^{11}B(α,n)^{14}N and at higher temperatures ^{7}Be(α,γ)^{11}C(p,γ)^{12}N(β^{+})^{12}C. Both branches facilitate alternative break-out possibilities, however without the production of the important deuterons as fuel for the hot pp-chains.

The ^{10}B(p,α)^{7}Be reaction has been extensively studied over a wide energy range between 20 keV and 2 MeV using a number of different accelerator facilities (see Wiescher et al. [18] and references therein). The reaction cross section is considerably larger than the competing ^{10}B(p,γ)^{11}C radiative capture reaction [19]. Figure 1 shows the S-factor for the transitions to the ground state and the first excited state in ^{7}Be. The astrophysical S-factor, $S(E)$, represents the energy dependent cross section $\sigma(E)$ of the reaction corrected in first order for the Coulomb penetrability. $S(E)$ therefore represents the nuclear transition probability as

well as the tunneling probability through the orbital momentum barrier as a function of the energy E.

$$S(E) = \sigma(E) \cdot E \cdot e^{2\pi\eta}, \quad (1)$$

with η being the classical Sommerfeld parameter.

The S-factor curve for the ^{10}B(p,α)^{7}Be reaction towards lower energies is characterized by the tail of a strong resonance at 10 keV [7, 22] and by the contribution of several broad and interfering resonances in the higher energy range [18]. The cross section determination is based on a comprehensive R-matrix analysis including representative sets of ^{10}B(p,α)^{7}Be data and also includes data for complementary reaction channels such as radiative capture ^{10}B(p,γ)^{11}C and elastic scattering ^{10}B(p,p)^{10}B as described by [14]. Through this self-consistent application of the phenomenological R-matrix theory [13], a reliable extrapolation over the entire energy range with relative small uncertainty has been achieved [43, 25].

2.1 R-matrix analysis of the ^{10}B(p,α)^{7}Be

As discussed above, the low energy cross section of the ^{10}B(p,α)^{7}Be reaction is dominated by a strong s-wave, near threshold, resonance at ≈10 keV. The corresponding level has a total width of ≈15 keV and has $J^{\pi} = 5/2^{+}$. There is a single direct experimental study that measures down to the very low energy of $E_{\text{c. m.}} = 17$ keV [22]. A more recent Trojan Horse measurement has also studied the very low cross section, reporting data down to 5 keV that maps the near threshold resonance [23]. Despite these low energy measurements, the cross section at the energies of inertial confinement fusion facilities still is rather uncertain. For example, Spitaleri et al. [25] quotes a low energy uncertainty of between 10 and 20%. While the data of Angulo et al. [22] have rather small error bars, the data also show a significant amount of scatter, indicating the presence of significant non-statistical uncertainties.

In addition, the near threshold $5/2^{+}$ resonance can interfere strongly with other higher energy resonances, which strongly motivates an R-matrix analysis that covers a broader energy range. The recent work of Vande Kolk et al. [14] provided a consistent set of ^{10}B(p,α)^{7}Be angular distribution data that resulted in a much improved characterization of the next highest energy $5/2^{+}$ resonance at ≈1.3 MeV, which has a total width of ≈740 keV and interferes strongly with the near threshold state.

It should be noted that the TUNL evaluation lists another $5/2^{+}$ state at $E_x = 9.200$ (50) keV, but in Vande Kolk et al. [14] no evidence for this state was found, so it has not been considered. Additionally, the large widths of the resonances in this region tend to obfuscate level identification. Microscopic calculations near the proton separation energy in ^{11}C would be very helpful in producing firmer level assignments.

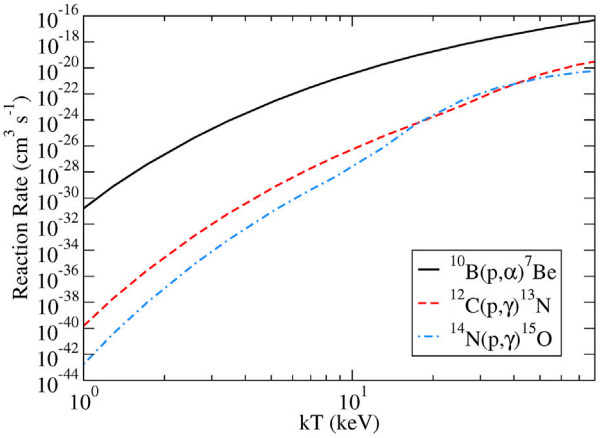

FIGURE 2
Reaction rates for the ^{10}B(p,α)^{7}Be (solid black line), ^{12}C(p,γ)^{13}N (dashed red line) and ^{14}N(p,γ)^{15}O (dashed-dotted blue line) reactions calculated from the R-matrix fits described throughout the remainder of the text.

2.2 The reaction rate of ^{10}B(p,α)^{7}Be

The reaction rate for a nuclear reaction process characterized by broad overlapping and interfering resonances is determined by numerical integration over the reaction cross section and Maxwell Boltzmann distribution of the interacting particles, with the factors $f(\rho)$, which corrects for electron screening, and the partition function $G(T)$, which takes into account the contribution of thermally excited states in a plasma environment

$$N_A\langle\sigma v\rangle = \left(\frac{8}{\pi\mu}\right)^{1/2} \frac{N_A}{(k_B T)^{3/2}} \int_0^{\infty} f(\rho) \cdot G(T) \cdot \sigma(E) \cdot E \cdot e^{-E/k_B T} dE. \quad (2)$$

Here N_A is Avogadro's number, k_B is the Boltzmann constant, T is the temperature, ρ is the density, and μ is the reduced mass. The reaction rate as a function of temperature is shown in Figure 2. The electron screening factor $f(\rho)$ depends on the density of the stellar environment [26] and is typically based on theoretical estimates based on assumptions on an additional screening potential term in the nuclear potential [27], while the partition function $G(T)$ is calculated as the probability for thermally populating excited states in a hot plasma [28], respectively. These two model dependent terms carry a substantial uncertainty, depending on the assumptions about the screening potential in the laboratory experiment and the plasma as well on the knowledge or assumptions on the excitation energies and level density of the target nucleus. The rate declines rapidly with temperature with the contributions of the broad resonance structures observed in the cross section (see Figure 1) determining the absolute value of the rate at each

temperature. The reaction rate measured directly at a laser plasma facility will differ from the reaction rate based on low energy accelerator experiments, which does not provide information about the screening factor and the partition function. A direct measurement of a reaction rate in a quasi-stellar plasma such as provided by Omega and NIF in comparison with accelerator based reaction rate estimates offers a unique way for experimentally determining these parameters.

The production of ^{7}Be in a laser driven hot plasma environment can be calculated from the reaction rate and the abundances of ^{10}B boron and ^{1}H hydrogen fuel. The difference between observed and predicted number of reaction products will provide the necessary information about the environmental parameters in a plasma environment.

The production rate of ^{7}Be is determined by

$$\frac{dN_{^7Be}}{dt} = N_{^{10}B} \cdot N_{^1H} \cdot \rho \cdot N_A \langle \sigma v \rangle_{^{10}B(p,\alpha)^7Be}. \quad (3)$$

This equation does not include any possible depletion reaction of ^{7}Be by either electron capture or radiative proton capture, since these processes are anticipated to have a much smaller reaction rate than the ^{10}B$(p,\alpha)^{7}$Be production rate.

2.3 The ^{7}Be production in a laser driven plasma environment

The production of ^{7}Be can be obtained by integrating the production rate over the temperature and density development in the laser driven plasma. The yield $Y_{^7Be}$ of ^{7}Be produced in a high temperature shot environment can be easily estimated in the framework of a simplified 1D hot spot model from the reaction rate per particle pair, the number densities $N_{^{10}B}$ and $N_{^1H}$ for the reaction partners in the plasma, boron and hydrogen, respectively, the hot spot volume V_{HS}, and the actual burn width Δt:

$$Y_{^7Be} = N_{^{10}B} \cdot N_{^1H} \cdot \langle \sigma v \rangle_{^{10}B(p,\alpha)^7Be} \cdot V_{HS} \cdot \Delta t. \quad (4)$$

For a NIF like laser driven plasma study of the reaction, the optimum gas filling of the capsule would be a$^{10}B_2H_6$ Di-Borane fill gas with number densities of $N_{^{10}B} \approx 10^{20}$ cm^{-3} and $N_{^1H} \approx 3 \cdot 10^{20}$ cm^{-3}, respectively. This would correspond to a rather high density after compression to a hot spot volume of about $V_{HS} \approx 10^{-6}$ cm^3 for the burn width period of $\Delta t \approx 10^{-10}$ s. From Figure 2, the reaction rate can be estimated to be $\langle \sigma v \rangle_{^{10}B(p,\alpha)^7Be} \approx 10^{-20}$ cm^{3}s^{-1} at a temperature of about $kt \approx 30$ keV. It should be noted that these temperature levels have so far only be reached in direct drive implosions, with the laser beams directly incident on the target [29]. Adopting these conditions results in a production yield of $Y_{^7Be} \approx 10^4$ to 10^{5}^{7}Be nuclei per shot. This number depends linearly on the amount of gas in the shot capsule, but exponentially on the temperature reached in the plasma during the shot since the reaction rate varies exponentially with temperature. Higher shot temperatures would certainly translate into a substantially higher ^{7}Be production.

This material must be collected either by catcher foils or by the cryogenic Radiochemical Analysis of Gaseous Samples (RAGS) system [30] to be analyzed and counted by high sensitivity mass separation or Accelerator Mass Spectrometry (AMS) techniques. The RAGS system so far has been only applied to the analysis of indirect drive implosions with a Hohlraum system and new developments are required for its application in direct drive implosions. Considering the low number of ^{7}Be isotopes produced during a single shot, their identification by measuring the characteristic 10% γ decay at 478 keV would not provide sufficient sensitivity for a successful counting experiment.

This is of course only a rather crude estimate of the production of ^{7}Be, a more reliable simulation would also require taking other reaction channels, such as ^{7}Be$(p,\gamma)^{8}$B, into account, which would reduce the production number. However, as this reaction cross section is orders of magnitude smaller, it can be neglected in the present calculations.

3 The ^{12}C$(p,\gamma)^{13}$N reaction

The ^{12}C$(p,\gamma)^{13}$N reaction is an important link in the so-called CNO cycle, which facilitates stellar hydrogen burning in massive stars. The CNO cycle is a catalytic process that is based on the capture of four protons on the existing abundance of carbon, nitrogen, and also oxygen isotopes in a stellar environment with the subsequent emission of one alpha particle as well as two positrons ^{12}C$(p,\gamma)^{13}$N$(\beta^{+}\nu)^{13}$C$(p,\gamma)^{14}$N$(p,\gamma)^{15}$O$(\beta^{+}\nu)^{15}$N$(p,\alpha)^{12}$C [31]. The CNO cycle is not only important as an energy source for massive stars but it also contributes to the production of CNO neutrinos in our sun [32].

In the CNO reaction sequence, the ^{12}C$(p,\gamma)^{13}$N reaction plays an important role in determining the fate of the ^{12}C isotope in an hydrogen burning environment as well for the production of ^{13}N. The β^{+} decay of ^{13}N is one of the predicted CNO neutrino sources, whose strength is defined by the ^{12}C$(p,\gamma)^{13}$N capture rate since the production and the ^{13}N decay are in equilibrium. This shows that the respective neutrino emission rate $A_\nu(^{13}N)$ depends directly on the ^{12}C$(p,\gamma)^{13}$N reaction rate $N_A\langle \sigma v \rangle_{^{12}C(p,\gamma)^{13}N}$ and the abundances of ^{12}C and ^{1}H in the solar core:

$$A_\nu(^{13}N) = \frac{dN_{^{13}N}}{dt} = N_{^{12}C} \cdot N_{^1H} \cdot \rho \cdot N_A \langle \sigma v \rangle_{^{12}C(p,\gamma)^{13}N}. \quad (5)$$

To reliably evaluate the ^{13}N component in the solar CNO neutrino flux a reliable reaction rate for the ^{12}C$(p,\gamma)^{13}$N reaction in a plasma environment is necessary. This however presents a major challenge because of the low reaction cross section.

The ^{12}C$(p,\gamma)^{13}$N reaction is a radiative capture process, which is based on the electromagnetic interaction, rather than the

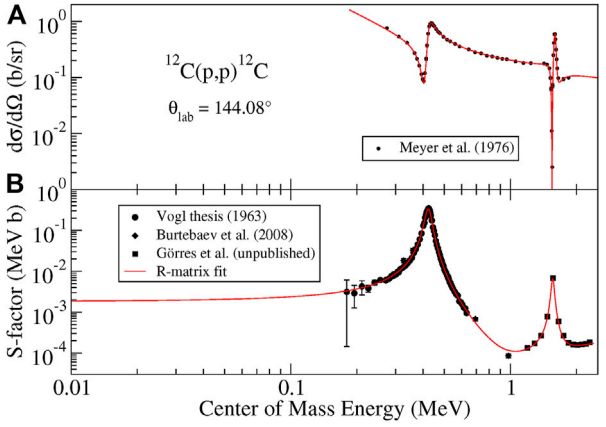

FIGURE 3
Simultaneous *R*-matrix fit to **(A)** the differential cross section data of Meyer et al. [34], **(B)** the $^{12}C(p,\gamma)^{13}N$ angle integrated data of Vogl [35] and Burtebaev et al. [36] as well as the differential cross section data of Rolfs and Azuma [33], with adjustments for energy calibration.

strong interaction, in contrast to our previous example. For this reason, the cross section is expected to be substantially weaker. However, at low energies, the $^{12}C(p,\gamma)^{13}N$ reaction is characterized by the contributions from two pronounced resonances and a non-resonant direct capture mechanism as well as possible interference between these reaction components [33]. The strength of these components define the low energy cross section of the reaction and therefore also the reaction rate. Figure 3 shows the *S*-factor of the $^{12}C(p,\gamma)^{13}N$ reaction at low energies characterized by the contributions of the two broad low energy resonances including new and as yet unpublished data in the energy range above 1 MeV to obtain a better handle on the upper resonance. The solid line presents a new *R*-matrix analysis of the reaction cross section as described in the following.

3.1 *R*-matrix analysis of $^{12}C(p,\gamma)^{13}N$

The $^{12}C(p,\gamma)^{13}N$ reaction is ideally suited for an *R*-matrix description. Only a single, broad, *s*-wave resonance contributes to the low energy cross section at $E_{c.m.} = 461$ keV. As shown in Azuma et al. [13], the low energy cross section can be described very well by the interference of this broad resonance with *E*1 direct capture, modeled with external capture [5, 11, 37]. The exceptional data of Vogl [35] carefully map this low energy resonance. These data have been found to be consistent with the recent measurements of Burtebaev et al. [36]. The reaction was also studied by Rolfs and Azuma [33], but was found to have issues with its energy calibration [40]. The *R*-matrix fit is found to give an excellent reproduction of the data and the extrapolation of the low energy cross section is quoted as having an uncertainty of ≈18% [13], which is largely dominated by the overall normalization uncertainty.

3.2 The ^{13}N production in a laser driven plasma environment

The measurement of $^{12}C(p,\gamma)^{13}N$ in a laser driven plasma environment is a considerable challenge because of the overall low reaction rate at the characteristic conditions of a NIF shot where

$$Y_{^{13}N} = N_{^{12}C} \cdot N_{^{1}H} \cdot \langle \sigma v \rangle_{^{12}C(p,\gamma)^{13}N} \cdot V_{HS} \cdot \Delta t. \quad (6)$$

For a gas filled capsule, methane $^{12}CH_4$ seems to be a suitable choice with a particle densities of $N_{^{12}C} \approx 10^{20}$ cm^{-3} and $N_{^{1}H} \approx 4 \cdot 10^{20}$ cm^{-3}, respectively. The reaction rate at $kT \approx 30$ keV is $\langle \sigma v \rangle_{^{12}C(p,\gamma)^{13}N} \approx 2 \cdot 10^{-24}$ cm^{3}s^{-1}, approximately four orders of magnitude weaker than the rate of the $^{10}B(p,\alpha)^7Be$ strong interaction process. This translates, at comparable shot conditions, into six orders of magnitude lower yield, $Y_{^{13}N} \approx 10$ ^{13}N nuclei per shot. Considering the presently available shot rate of less than 10 shots per day, these are obviously insufficient conditions for a laser plasma experiment. This yield can be enhanced by some factor by increasing the concentration of the reaction components either by using higher filling pressure or exchanging methane CH_4 by butane C_4H_{10} gas. The Significantly higher shot temperatures need to be reached to obtain a measurable ^{13}N yield.

The relatively short half-life of ^{13}N, $t_{1/2} = 9.97$ min, provides another obstacle since it requires a speedy removal of the reaction products from the NIF environment. Identification and analysis of an on-line AMS or PET microlensing system, as developed for mapping microdoses of radioactivity in pharmaceutical studies [42, 41], could be used. Yet, it remains doubtful if such spurious amounts of characteristic ^{13}N can be collected and filtered out of the relatively dirty vacuum environment of present generation plasma facilities.

4 The $^{14}N(p,\gamma)^{15}O$ reaction

The $^{14}N(p,\gamma)^{15}O$ reaction has been identified as the slowest reaction in the CNO cycles [31]. The reaction includes several sizable transitions to both the ground state and higher excited states and is characterized by non-resonant direct capture contributions as well as contributions from the tails of higher energy resonances [31, 43] interfering with the high energy tails of different subthreshold states [45]. The reaction rate is determined by the sum of all of these transitions at the temperature of the stellar or laboratory hydrogen burning environment. The $^{14}N(p,\gamma)^{15}O$ reaction results in the production of ^{15}O, which β^+ decays, also emitting a neutrino at fairly high energies. Recent measurements of the BOREXINO detector showed signatures of the neutrino flux associated with the ^{15}O decay [46]. The observed neutrino rate $A_\nu(^{15}O)$ seems to be slightly higher than suggested by the reaction rate $N_A\langle \sigma v \rangle_{^{14}N(p,\gamma)^{15}O}$ based on accelerator data

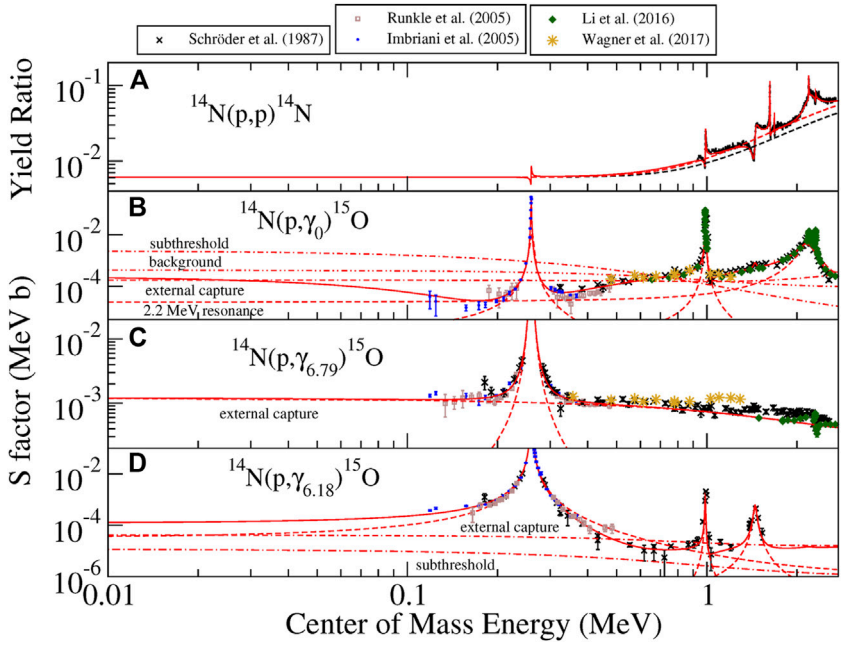

FIGURE 4
Simultaneous *R*-matrix fit to **(A)** the ^{14}N(*p*,*p*)^{14}N data of deBoer et al. [48] and the ^{14}N(*p*,*γ*)^{15}O data of Schröder et al. [49], Runkle et al. [50], Imbriani et al. [43], Li et al. [44], Wagner et al. [51] for the ground state **(B)**, 6.79 MeV **(C)**, and 6.18 MeV **(D)** excited states.

$$A_\gamma(^{15}O) = \frac{dN_{^{15}O}}{dt} = N_{^{14}N} \cdot N_{^{1}H} \cdot \rho \cdot N_A \langle \sigma v \rangle_{^{14}N(p,\gamma)^{15}O}. \quad (7)$$

This might either suggest a higher abundance of $N_{^{14}N}$ or a change in the reaction rate. The latter, however, was confirmed by a new reaction study [15]. The following section provides a short summary of the nuclear physics of the reaction as reflected in the *R*-matrix analysis of the reaction channels.

4.1 *R*-matrix analysis of ^{14}N(*p*,*γ*)^{15}O

There are three transitions that dominate the total capture cross section for the ^{14}N(*p*,*γ*)^{15}O reaction: the 6.79 MeV, ground state, and 6.17 MeV [47] (as shown in Figure 4). The 6.79 MeV transition is described well by pure hard sphere external capture [44]. The 6.17 MeV transition is instead dominated by the tail of the 278 keV resonance at low energies. In constrast, the ground state transition data, especially the very low energy measurements of Imbriani et al. [43], have proven to be very challenging to describe, especially when analyzed simultaneously with higher energy data [21, 16, 44]. The low energy cross section for this transition is made up of contributions from the 278 keV resonance, external capture, at least one subthreshold state, and the low energy tail of broad higher energy resonances [48]. The complications of obtaining a satisfactory *R*-matrix description of this transition are summarized in Frentz et al. [15] and Gyürky et al. [52]. Despite the difficulties in describing the ground state transition, the low energy cross section is thought to have a relatively small uncertainty of ≈7% [47].

4.2 The ^{15}O production in a laser driven plasma environment

A measurement of the reaction in a plasma would be extremely interesting to investigate the possibility of plasma related changes in the reaction rate. The reaction rate at $kT \approx 30$ keV is $\langle \sigma v \rangle_{^{14}N(p,\gamma)^{15}O} \approx 3.5 \cdot 10^{-24}$ cm^{3}s^{-1}, which is comparable to the reaction rate of ^{12}C(p,*γ*)^{13}N. The best target gas might be an ammonia gas NH_3 or a mixture of N_2 and H_2. Adopting an ammonium gas, particle densities of $N_{^{14}N} \approx 10^{20}$ cm^{-3} and $N_{^{1}H} \approx 3 \cdot 10^{20}$ cm^{-3} are obtained, respectively. This translates, for comparable shot conditions as described above, into a yield of $Y_{^{15}O} \approx 10$ ^{15}O nuclei per shot, comparable to the anticipated count rate for the ^{12}C(*p*,*γ*)^{13}N reaction.

Again, the low production rate of the adopted shot conditions makes an experimental study of radiative capture reactions challenging. Higher densities would be desirable to improve the conditions for a direct study of such a reaction in a laser plasma experiment. An additional technical challenge is the half life of ^{15}O, $t_{1/2} = 2.01$ min, considerably shorter than that of ^{13}N; this requires the development of speedy high efficiency extraction methods.

5 Conclusion

Three reactions have been analyzed on their suitability for study at laser confined plasma facilities such as NIF or Omega. These studies would be important as a direct way to explore the screening of the deflecting Coulomb barrier in a charged particle fusion or capture process at the conditions of a stellar plasma. While a number of reactions have been studied for fusion between light hydrogen and helium isotopes [52, 23, 2], no studies exist for these kind of reactions for higher Z nuclei. The more recent measurement of $^{10}B(\alpha,n)^{13}N$ was a promising first step [10], however, the technique was not quite suitable for the study of reactions at stellar burning conditions. The boron content was part of the outer beryllium ablator containing a 65/35 % deuterium–tritium (DT) gas fill. The α particles were produced by D+T fusion reactions and therefore had a much higher energy than α particles in a thermal plasma. The successful analysis of the ^{13}N reaction products using RAGS, however, demonstrated that such measurements remain feasible.

The $^{10}B(p,\alpha)^{7}Be$, $^{12}C(p,\gamma)^{13}N$, and the $^{14}N(p,\gamma)^{15}O$ reactions are suitable because the radioactive decay of the reaction products provide a unique signature. In addition, these reactions play an important role in astrophysics, from the nucleosynthesis in first stars to the interpretation of the CNO neutrino flux from our sun. The cross section data derived from accelerator based reaction data have been extrapolated into the energy range of the plasma environment by a extensive R-matrix analyses, taking into account many reaction channels. The reaction yield produced in a generic NIF shot has been estimated on the basis of these reaction cross sections. The results indicate that the production rate is limited by the low cross sections compared to the fusion reactions with lower Z nuclei. The strong interaction $^{10}B(p,\alpha)^{7}Be$ process is the most promising, not only is the reaction cross section much higher than the typical one for radiative capture reactions such as $^{12}C(p,\gamma)^{13}N$ and the $^{14}N(p,\gamma)^{15}O$, but also because of the lower Z of the isotopes involved. Without significant improvement in the experimental arrangements, the chances for measuring reactions with higher Z isotopes are limited.

Data availability statement

Publicly available datasets were analyzed in this study. This data can be found here: https://www-nds.iaea.org/exfor/.

Author contributions

MW, RD, and JG contributed to the conception of this research. MW and JG made the NIF yield calculations and RD provided the cross sections and reaction rates. MW wrote the first draft of the manuscipt and RD and JG edited and contributed to sections of the manuscipt. All authors contributed to the final editting and revision of the manuscipt and approved it for submission.

Funding

This research utilized resources from the Notre Dame Center for Research Computing and was funded by the National Science Foundation through Grant No. PHY-2011890 (University of Notre Dame Nuclear Science Laboratory), Grant No. PHY-1430152 (the Joint Institute for Nuclear Astrophysics—Center for the Evolution of the Elements).

Conflict of interest

The authors declare that the research was conducted in the absence of any commercial or financial relationships that could be construed as a potential conflict of interest.

Publisher's note

All claims expressed in this article are solely those of the authors and do not necessarily represent those of their affiliated organizations, or those of the publisher, the editors and the reviewers. Any product that may be evaluated in this article, or claim that may be made by its manufacturer, is not guaranteed or endorsed by the publisher.

References

1. Assenbaum HJ, Langanke K, Rolfs C. Low-energy $^{2}H(d,\gamma)^{4}He$ reaction and the d-state admixture in the ^{4}He ground state. *Phys Rev C* (1987) 36:17–20. doi:10.1103/PhysRevC.36.17

2. Sayre DB, Brune CR, Caggiano JA, Glebov VY, Hatarik R, Bacher AD, et al. Measurement of the $T + T$ neutron spectrum using the national ignition facility. *Phys Rev Lett* (2013) 111:052501. doi:10.1103/PhysRevLett.111.052501

3. Gatu Johnson M, Forrest CJ, Sayre DB, Bacher A, Bourgade J-L, Brune CR, et al. Experimental evidence of a variant neutron spectrum from the $T(t, 2n)\alpha$ reaction at center-of-mass energies in the range of 16–50 keV. *Phys Rev Lett* (2018) 121:042501. doi:10.1103/PhysRevLett.121.042501

4. Zylstra AB, Frenje JA, Gatu Johnson M, Hale GM, Brune CR, Bacher A, et al. Proton spectra from $^{3}He + T$ and $^{3}He + ^{3}He$ fusion at low center-of-mass energy, with potential implications for solar fusion cross sections. *Phys Rev Lett* (2017) 119:222701. doi:10.1103/PhysRevLett.119.222701

5. Nuckolls J, Wood L, Thiessen A, Zimmerman G. Laser compression of matter to super-high densities: Thermonuclear (CTR) applications. *Nature* (1972) 239:139–42. doi:10.1038/239139a0

6. Edwards MJ, Patel PK, Lindl JD, Atherton LJ, Glenzer SH, Haan SW, et al. Progress towards ignition on the national ignition facility. *Phys Plasmas* (2013) 20:070501. doi:10.1063/1.4816115

7. Boehly T, Brown D, Craxton R, Keck R, Knauer J, Kelly J, et al. Initial performance results of the omega laser system. *Opt Commun* (1997) 133:495–506. doi:10.1016/S0030-4018(96)00325-2

8. Cerjan CJ, Bernstein L, Hopkins LB, Bionta RM, Bleuel DL, Caggiano JA, et al. Dynamic high energy density plasma environments at the National Ignition Facility for nuclear science research. *J Phys G: Nucl Part Phys* (2018) 45:033003. doi:10.1088/1361-6471/aa8693

9. Liu Q, Febbraro M, deBoer RJ, Aguilar S, Boeltzig A, Chen Y, et al. Low-energy cross-section measurement of the ^{10}B(α,n)^{13}N reaction and its impact on neutron production in first-generation stars. *Phys Rev C* (2020) 101:025808. doi:10.1103/PhysRevC.101.025808

10. Lonardoni D, Sauppe JP, Batha SH, Birge N, Bredeweg T, Freeman M, et al. First measurement of the ^{10}B(α,n)^{13}N reaction in an inertial confinement fusion implosion at the National Ignition Facility: Initial steps toward the development of a radiochemistry mix diagnostic. *Phys Plasmas* (2022) 29:052709. doi:10.1063/5.0079676

11. Lane AM, Thomas RG. R-matrix theory of nuclear reactions. *Rev Mod Phys* (1958) 30:257–353. doi:10.1103/RevModPhys.30.257

12. Descouvemont P, Baye D. The *R*-matrix theory. *Rep Prog Phys* (2010) 73:036301. doi:10.1088/0034-4885/73/3/036301

13. Azuma RE, Uberseder E, Simpson EC, Brune CR, Costantini H, de Boer RJ, et al. Azure: An *R*-matrix code for nuclear astrophysics. *Phys Rev C* (2010) 81:045805. doi:10.1103/PhysRevC.81.045805

14. Vande Kolk B, Macon KT, deBoer RJ, Anderson T, Boeltzig A, Brandenburg K, et al. Investigation of the ^{10}B(p,α)^{7}Be reaction from 0.8 to 2 0 MeV. *Phys Rev C* (2022) 105:055802. doi:10.1103/PhysRevC.105.055802

15. Frentz B, Aprahamian A, Boeltzig A, Clark A, deBoer R, Gilardy G, et al. (2022). Investigation of the ^{14}N(p,γ)^{15}O reaction for the CNO cycle (PRC in print).

16. Wiescher M, Clarkson O, deBoer RJ, Denisenkov P. Nuclear clusters as the first stepping stones for the chemical evolution of the universe. *Eur Phys J A* (2021) 57:24. doi:10.1140/epja/s10050-020-00339-x

17. Wiescher M, Gorres J, Graff S, Buchmann L, Thielemann FK. The hot proton-proton chains in low-metallicity objects. *ApJ* (1989) 343:352. doi:10.1086/167709

18. Wiescher M, deBoer RJ, Görres J, Azuma RE. Low energy measurements of the ^{10}B(p,α)^{7}Be reaction. *Phys Rev C* (2017) 95:044617. doi:10.1103/PhysRevC.95.044617

19. Wiescher M, Boyd RN, Blatt SL, Rybarcyk LJ, Spizuoco JA, Azuma RE, et al. ^{11}C level structure via the ^{10}B(p,γ) reaction. *Phys Rev C* (1983) 28:1431–42. doi:10.1103/PhysRevC.28.1431

20. Chiari M, Giuntini L, Mandò P, Taccetti N. Proton elastic scattering cross-section on boron from 0.5 to 3.3 MeV. *Nucl Instr Methods Phys Res Section B: Beam Interactions Mater Atoms* (2001) 184:309–18. doi:10.1016/S0168-583X(01)00787-X

21. Youn M, Chung H, Kim J, Bhang H, Chung K-H. The ^{10}B(p,α_0)^{7}Be reaction in the thermonuclear energy region. *Nucl Phys A* (1991) 533:321–32. doi:10.1016/0375-9474(91)90493-P

22. Angulo C, Engstler S, Raimann G, Rolfs C, Schulte WH, Somorjai E. The effects of electron screening and resonances in (p, α) reactions on ^{10}B and ^{11}B at thermal energies. *Z Physik A - Hadrons Nuclei* (1993) 345:231–42. doi:10.1007/BF01293350

23. Spitaleri C, Lamia L, Puglia SMR, Romano S, La Cognata M, Crucillà V, et al. Measurement of the 10 keV resonance in the ^{10}B(p,α_0)^{7}Be reaction via the Trojan Horse method. *Phys Rev C* (2014) 90:035801. doi:10.1103/PhysRevC.90.035801

24. Angulo C, Schulte WH, Zahnow D, Raimann G, Rolfs C. Astrophysical $S(E)$ factor of ^{10}B(p,α_1)^{7}Be at low energies. *Z Physik A - Hadrons Nuclei* (1993) 345:333–4. doi:10.1007/BF01280844

25. Spitaleri C, Puglia SMR, La Cognata M, Lamia L, Cherubini S, Cvetinović A, et al. Measurement of the ^{10}B(p,α_0)^{7}Be cross section from 5 keV to 1.5 MeV in a single experiment using the Trojan horse method. *Phys Rev C* (2017) 95:035801. doi:10.1103/PhysRevC.95.035801

26. Gasques LR, Afanasjev AV, Aguilera EF, Beard M, Chamon LC, Ring P, et al. Nuclear fusion in dense matter: Reaction rate and carbon burning. *Phys Rev C* (2005) 72:025806. doi:10.1103/PhysRevC.72.025806

27. Assenbaum HJ, Langanke K, Rolfs C. Effects of electron screening on low-energy fusion cross sections. *Z Physik A - At Nuclei* (1987) 327:461–8. doi:10.1007/BF01289572

28. Fowler WA, Caughlan GR, Zimmerman BA. Thermonuclear reaction rates, ii. *Annu Rev Astron Astrophys* (1975) 13:69–112. doi:10.1146/annurev.aa.13.090175.000441

29. Jeet J, Zylstra AB, Gatu-Johnson M, Kabadi NV, Adrian P, Forrest C, et al. (2022). Development of a platform for studying solar CNO reactions in an ICF plasma.

30. Shaughnessy DA, Velsko CA, Jedlovec DR, Yeamans CB, Moody KJ, Tereshatov E, et al. The radiochemical analysis of gaseous Samples (RAGS) apparatus for nuclear diagnostics at the national ignition facility (invited). *Rev Scientific Instr* (2012) 83:10D917. doi:10.1063/1.4742145

31. Wiescher M, Görres J, Uberseder E, Imbriani G, Pignatari M. The cold and hot i404. doi:10.1146/annurev.nucl.012809.104505

32. Haxton W, Hamish Robertson R, Serenelli AM. Solar neutrinos: Status and prospects. *Annu Rev Astron Astrophys* (2013) 51:21–61. doi:10.1146/annurev-astro-081811-125539

33. Rolfs C, Azuma R. Interference effects in ^{12}C(p,γ)^{13}N and direct capture to unbound states. *Nucl Phys A* (1974) 227:291–308. doi:10.1016/0375-9474(74)90798-2

34. Meyer H, Plattner G, Sick I. Elastic p+^{12}C scattering between 0.3 and 2 MeV. *Z Physik A* (1976) 279:41–5. doi:10.1007/BF01409090

35. Vogl JL. Radiative capture of protons by 12C and 13C below 700 keV. Ph.D. thesis. Pasadena, CA, United States: California Institute of Technology (1963).

36. Burtebaev N, Igamov SB, Peterson RJ, Yarmukhamedov R, Zazulin DM. New measurements of the astrophysical *S* factor for ^{12}C(p,γ)^{13}N reaction at low energies and the asymptotic normalization coefficient (nuclear vertex constant) for the p + ^{12}C $\rightarrow$^{13}N reaction. *Phys Rev C* (2008) 78:035802. doi:10.1103/PhysRevC.78.035802

37. Holt RJ, Jackson HE, Laszewski RM, Monahan JE, Specht JR. Effects of channel and potential radiative transitions in the ^{17}O(γ, n_0)^{16}O reaction. *Phys Rev C* (1978) 18:1962–72. doi:10.1103/PhysRevC.18.1962

38. Barker FC, Kajino T. The ^{12}C(α,γ)^{16}O cross section at low energies. *Aust J Phys* (1991) 44:369–96. doi:10.1071/PH910369

39. Angulo C, Descouvemont P. The ^{14}N(p,γ)^{15}O low-energy *S*-factor. *Nucl Phys A* (2001) 690:755–68. doi:10.1016/S0375-9474(00)00696-5

40. Angulo C, Arnould M, Rayet M, Descouvemont P, Baye D, Leclercq-Willain C, et al. A compilation of charged-particle induced thermonuclear reaction rates. *Nucl Phys A* (1999) 656:3–183. doi:10.1016/S0375-9474(99)00030-5

41. Lappin G, Garner R. Big physics, small doses: The use of ams and pet in human microdosing of development drugs. *Nat Rev Drug Discov* (2003) 2:233–40. doi:10.1038/nrd1037

42. Turteltaub K, Vogel J. Bioanalytical applications of accelerator mass spectrometry for pharmaceutical research. *Curr Pharm Des* (2000) 6:991–1007. doi:10.2174/1381612003400047

43. Imbriani G, Costantini H, Formicola A, Bemmerer D, Bonetti R, Broggini C, et al. The bottleneck of CNO burning and the age of Globular Clusters. *Astron Astrophys* (2004) 420:625–9. doi:10.1051/0004-6361:20040981

44. Li Q, Görres J, deBoer RJ, Imbriani G, Best A, Kontos A, et al. Cross section measurement of ^{14}N(p,γ)^{15}O in the CNO cycle. *Phys Rev C* (2016) 93:055806. doi:10.1103/PhysRevC.93.055806

45. Frentz B, Aprahamian A, Clark AM, Deboer RJ, Dulal C, Enright JD, et al. Lifetime measurements of excited states in ^{15}O. *Phys Rev C* (2021) 103:045802–10. doi:10.1103/PhysRevC.103.045802

46. Agostini M, Altenmüller K, Appel S, Atroshchenko V, Bagdasarian Z, Basilico D, et al. Experimental evidence of neutrinos produced in the CNO fusion cycle in the Sun. *Nature* (2020) 587:577–82. doi:10.1038/s41586-020-2934-0

47. Adelberger E, García A, Hamish Robertson R, Snover K, Balantekin A, Heeger KM, et al. Solar fusion cross sections. II. Theppchain and CNO cycles. *Rev Mod Phys* (2011) 83:195–245. doi:10.1103/RevModPhys.83.195

48. deBoer RJ, Bardayan DW, Görres J, LeBlanc PJ, Manukyan KV, Moran MT, et al. Low energy scattering cross section ratios of ^{14}N(p,p)^{14}N. *Phys Rev C* (2015) 91:045804. doi:10.1103/PhysRevC.91.045804

49. Schröder U, Becker H, Bogaert G, Görres J, Rolfs C, Trautvetter HP, et al. Stellar reaction rate of ^{14}N(p,γ)^{15}O and hydrogen burning in massive stars. *Nucl Phys A* (1987) 467:240–60. doi:10.1016/0375-9474(87)90528-8

50. Runkle RC, Champagne AE, Angulo C, Fox C, Iliadis C, Longland R, et al. Direct measurement of the ^{14}N(p,γ)^{15}O *S* factor. *Phys Rev Lett* (2005) 94:082503. doi:10.1103/PhysRevLett.94.082503

51. Wagner L, Akhmadaliev S, Anders M, Bemmerer D, Caciolli A, Gohl S, et al. Astrophysical *S* factor of the ^{14}N(p,γ)^{15}O reaction at 0.4-1.3 MeV. *Phys Rev C* (2018) 97:015801–15. doi:10.1103/PhysRevC.97.015801

52. Gyürky G, Halász Z, Kiss GG, Szücs T, Fülöp Z. Activation cross section measurement of the ^{14}N(p,γ)^{15}O astrophysical key reaction. *Phys Rev C* (2022) 105:L022801. doi:10.1103/PhysRevC.105.L022801